AGU ADVANCING EARTH AND SPACE SCIENCES

Geophysical Research Letters®

RESEARCH LETTER
10.1029/2023GL106451

Mixing of Rain and River Water in the Bay of Bengal From Basin-Scale Freshwater Balance

Sreelekha Jarugula[1,2], Debasis Sengupta[2,3], Emily Shroyer[4], and Fabrice Papa[5]

[1]Jet Propulsion Laboratory, California Institute of Technology, Pasadena, CA, USA, [2]Centre for Atmospheric and Oceanic Sciences, Indian Institute of Science, Bangalore, India, [3]International Centre for Theoretical Sciences (ICTS), Bangalore, India, [4]Office of Naval Research, Arlington, VA, USA, [5]Université de Toulouse, LEGOS (IRD/CNES/CNRS/UT3), Toulouse, France

Abstract We construct freshwater balance in the Bay of Bengal (BoB) within a control volume (CV) bounded by 1,018 kg/m^3 isopycnal surface using observations and ocean reanalysis during 2011–2015. Freshwater in CV is maximum in October–November due to monsoonal rain and river inflows, and minimum in April–May. Water lighter than 1,018 kg/m^3 is not transported out of BoB, implying that freshwater lost from CV is mixed away entirely within the basin. From freshwater budget, we infer moderate diapycnal mixing rates ($\sim 0.8 \times 10^{-5}$ m^2/s) in boreal spring and summer; in winter (December–January), the rate of freshwater loss to subsurface ocean is 0.015 m/day, corresponding to a median turbulent diffusivity of 4.2×10^{-5} m^2/s, with standard error of 25%. We show that enhanced winter mixing across the shallow pycnocline is due to reduced shortwave radiation and subseasonal episodes of surface buoyancy loss when cool, dry northeast monsoon winds blow over BoB.

Plain Language Summary The freshwater from monsoonal rivers and rain discharged into the Bay of Bengal (BoB) forms a shallow (<10 m deep) salinity-stratified layer which has implications for the regional air-sea interaction. There is very limited understanding of the mixing of the freshwater owing to the absence of near-surface turbulence measurements in BoB. It is important to understand the disappearance of the shallow fresh layer in the Bay due to it's linkages to the regional hydrological cycle and the near-surface stratification. In this study, we infer the seasonality of basin-scale mixing beneath the surface layer of BoB from a freshwater volume balance using a combination of observations and ocean analysis. We find that the highest rates of freshwater mixing (mean and median values of about 5.5×10^{-5} m^2/s and 4.2×10^{-5} m^2/s) occur during winter (December–January), mainly driven by enhanced surface buoyancy loss thereby reducing the freshwater content at a mean rate of 0.015 m/day. This study has implications for improvement of ocean and climate models, which generally have too-high mixing rates and poor representation of the salinity-stratified near-surface layer in BoB.

Key Points:

- Low-salinity water from monsoon rain and rivers covers nearly 80% of the northern Bay of Bengal's surface in October–November, and nearly vanishes by April–May
- The freshest (salinity <30 pss) and lightest (density <1,018 kg/m^3) water is not transported across the southern boundary, indicating modification or storage within the bay
- Freshwater balance shows that most of the rain and river water is mixed across the 1,018 kg/m^3 isopycnal surface in winter during episodes of enhanced surface buoyancy loss

Supporting Information:

Supporting Information may be found in the online version of this article.

Correspondence to:

S. Jarugula,
jslekha@gmail.com

Citation:

Jarugula, S., Sengupta, D., Shroyer, E., & Papa, F. (2024). Mixing of rain and river water in the Bay of Bengal from basin-scale freshwater balance. *Geophysical Research Letters*, *51*, e2023GL106451. https://doi.org/10.1029/2023GL106451

Received 22 SEP 2023
Accepted 28 DEC 2023

Author Contributions:

Data curation: Sreelekha Jarugula
Formal analysis: Sreelekha Jarugula
Investigation: Sreelekha Jarugula
Methodology: Sreelekha Jarugula
Validation: Sreelekha Jarugula
Visualization: Sreelekha Jarugula
Writing – original draft: Sreelekha Jarugula

1. Introduction

Small-scale ocean mixing processes leading to diffusion of heat, salt and other tracers across density surfaces, are closely tied to the energetics of the global ocean circulation (Gregg et al., 2018; Moum, 2021; Munk & Wunsch, 1998). Small-scale physical processes in the upper ocean determine the evolution of upper ocean temperature, salinity and density stratification in response to surface winds, and air-sea fluxes of heat and freshwater (Moum & Smyth, 2001). Air-sea interaction over the fresh, warm upper layer of the Bay of Bengal (BoB) favors multi-scale organization of monsoon convection (Bhat et al., 2001; Fu et al., 2007; Gadgil, 2003; Lau et al., 2012; Samanta et al., 2018; Vecchi & Harrison, 2002; Webster, 2006), and rapid intensification of tropical cyclones (Balaguru et al., 2012; Chaudhuri et al., 2019; Neetu et al., 2012). The aim of this study is to infer the seasonality of basin-scale mixing beneath the surface layer of BoB.

The BoB gains nearly 1.6 m (~4,000 km^3) of freshwater every year from monsoonal rivers and precipitation minus evaporation (P-E) during June–September (Sengupta et al., 2006; Papa et al., 2012). River water is stirred into the basin interior by mesoscale eddies and swift Ekman currents (Chaudhuri et al., 2021; Sreelekha et al., 2018, 2020). The area covered by fresh, light water with surface salinity <30 pss and density <1,018 kg/m^3 is highest in October–November, and approaches zero by April–May (Figure 1). In summer and autumn, the northern bay has a shallow (~5–10 m) fresh mixed layer and warm, salinity-stratified "barrier" layer, with subsurface pockets of trapped heat (Shroyer et al., 2021; Thadathil et al., 2016; Vinayachandran et al., 2002).

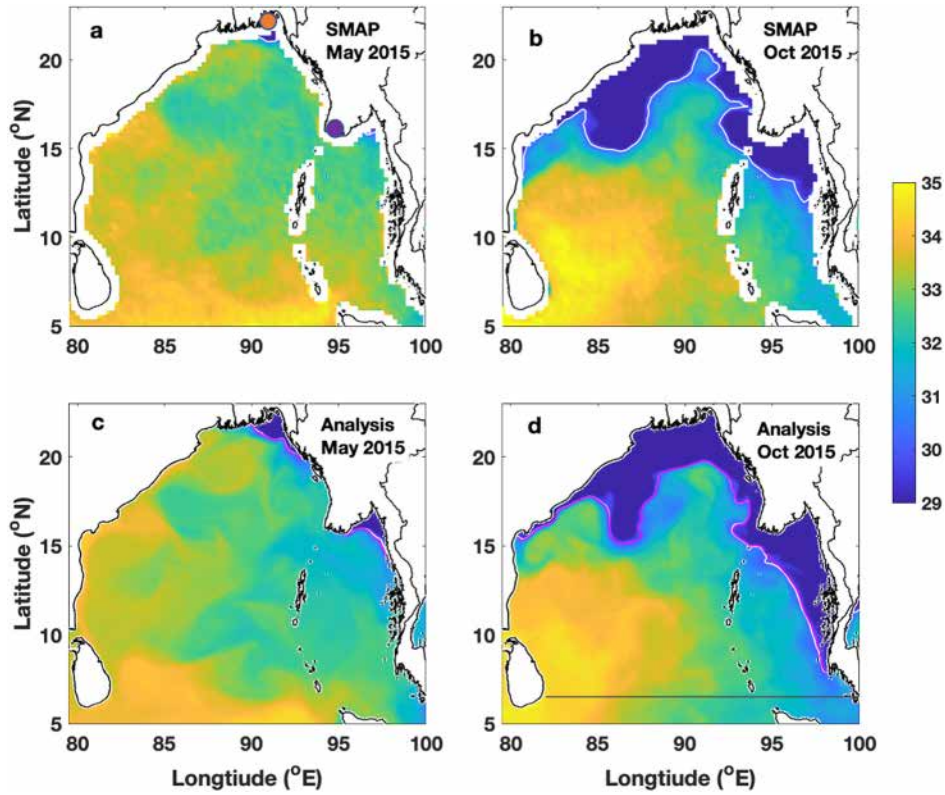

Figure 1. Bay of Bengal mean sea surface salinity (pss; color) from SMAP satellite in (a) May and (b) October of 2015. Mean salinity at 0.5 m depth (pss; color) from Global Ocean Analysis, in 2015 (c) May and (d) October. Ganga-Brahmaputra-Meghna (GBM; orange dot) and Irrawaddy (purple dot) river mouths are marked in (a). 30 pss contour (white curve) and 18 kg/m^3 potential density contour (magenta curve) at 0.5 m depth from the ocean analysis in (c, d); southern boundary of the bay at 6.5°N (gray) shown in (d).

High-resolution measurements in the north bay (Mahadevan et al., 2016) reveal rapidly changing, intricately layered salinity, temperature and density stratification in the upper ocean. Turbulence microstructure measurements show very low thermal diffusivity K_T (median values less than 10^{-5} m/s^2) beneath the fresh (24–31 pss) near-surface layer in August–September 2015 (Lucas et al., 2016), with evidence of enhanced values at the edges of sub-mesoscale fronts (Adams et al., 2019). These observations indicate that the fresh surface layer effectively isolates the deeper ocean from surface forcing. Strengthening winds can lead to shear-induced deepening of the mixed layer by nearly 30 m at the onset of monsoon (Shroyer et al., 2021). Using Solo floats equipped with turbulence sensors called χ-pods, Shroyer et al. (2016) showed that in August–September 2015, upward mixing of stored heat from a warm subsurface layer initially offsets any sea surface temperature (SST) cooling under 100 W/m^2 of net surface heat loss. Eventually, turbulence erodes the weak barrier layer, and SST falls rapidly due to mixing with cool upper thermocline water.

Direct turbulence measurements spanning a few seasonal cycles have been recently made at selected locations in BoB (Warner et al., 2016). The southern BoB is a site of active mixing between surface fresh water and saltier subsurface water from the Arabian Sea in summer (George et al., 2019; Vinayachandran et al., 2013; Wijesekera et al., 2016). Cherian et al. (2020) use χ-pod data from moorings along 8°N to study seasonal dependence of diffusivity at 30–100 m depth. The data show (a) highest diffusivities ($\kappa \sim O(10^{-4})$ m^2/s) below the mixed layer during June–September, (b) elevated mixing due to near-inertial shear during storm passage, and (c) absence of turbulence (near-molecular κ values) in April–May, when surface wind forcing is weak. The seasonal cycle of mixing is rather different in northern and southern BoB. Mixing in the north bay is very sensitive to the presence of river water at the surface: Moored turbulence records at 18°N 89.5°E show a striking suppression of subsurface turbulence upon arrival of river water (Thakur et al., 2019)—the median diffusivity decreased from 10^{-4} m^2/s to 10^{-5} m^2/s after the arrival of river water in mid-July. Both surface salinity and diffusivity were found to remain low until November, despite passage of a cyclone.

Modeling studies (Akhil et al., 2014; Benshila et al., 2014; Wilson & Riser, 2016) suggest that vertical mixing of freshwater is a primary mechanism to restore basin-average salinity to higher values during pre-monsoon season. Wilson and Riser (2016) use an eddy-resolving HYCOM model to evaluate salt budget of the upper 30 m of BoB. They report a vertical diffusivity of 10^{-4} m^2/s during September-November; however, HYCOM salinity values are higher than 30 pss in the upper 30 m, an overestimate compared to Argo observations. Observation-based studies emphasize shear-induced mixing and a possibility that SST cooling resulting in surface buoyancy loss may drive subsurface mixing in BoB during winter (Thadathil et al., 2016). Jampana et al. (2018) use hourly moored observations in north BoB to show that perturbations of reduced stratification due to buoyancy loss are responsible for mixing in post-monsoon season, whereas both buoyancy and shear perturbations play a role in winter. Girishkumar et al. (2020) report elevated diffusivities in winter due to surface buoyancy forcing, based on analysis of moored observations.

The extent of very fresh (salinity <30 pss) and light water in the BoB rises and falls with seasons. We use this simple observation to infer seasonal dependence of spatially averaged mixing in the near-surface ocean. We construct freshwater balance within a control volume (CV) enclosed by the 1,018 kg/m^3 isopycnal surface (18 kg/m^3 potential density anomaly surface) using daily eddy-permitting ocean reanalysis, daily continental runoff, precipitation and evaporation estimates during 2011–2015. We present data and methodology in Section 2, main results deduced from freshwater balance in Section 3, summary in Section 4.

2. Data and Methods

We use daily salinity, temperature, potential density and ocean currents from global ocean physics analysis and forecast (GLOBAL_MULTIYEAR_PHY_001_030) with 1/12° horizontal resolution, 22 vertical levels in the upper 100 m to estimate the volume of freshwater in BoB during 2011–2015 (EU, 2023). Global ocean analysis uses v3.1 NEMO model with atmospheric forcing from European Centre for Medium-Range Weather Forecasts (ECMWF) to obtain a daily 10-day forecast and assimilate the altimeter data, in situ temperature and salinity vertical profiles from Argo, XBT and satellite-derived SST but not satellite salinity; the model configuration does not include tides (Chassignet et al., 2018); the model uses a turbulent kinetic energy (TKE) closure scheme (Blanke & Delecluse, 1993) to parameterize vertical mixing. Other data sets include: daily 0.25° gridded rainfall from the Tropical Rainfall Measuring Mission (TRMM) Multi-satellite Precipitation Analysis, 3B42v7 (Huffman et al., 2016); daily 0.25° heat fluxes at the ocean surface from TropFlux data set (Praveen Kumar et al., 2012); daily 0.5° gridded global continental discharge data (Jarugula & Decharme, 2023) from the Interactions between Soil, Biosphere and Atmosphere-Total Runoff Integrating Pathways (ISBA-CTRIP) land surface model (Decharme et al., 2012, 2019).

Mixed layer depth (MLD) from the ocean analysis is estimated as the depth where potential density exceeds the surface density by 0.125 kg/m^3.

2.1. Estimating Freshwater Volume and Net Freshwater Input Within 18 kg/m^3 Isopycnal

Freshwater volume (FWV) within a CV bounded by a selected isopycnal surface over surface area A is defined as:

$$\mathrm{FWV} = \int_A \mathrm{FWC}(x, y)\,\mathrm{dx}\,\mathrm{dy} \tag{1}$$

where the freshwater content (FWC) at each point (x, y) is defined as $\int_{-Z}^{0}\left[1 - \frac{S(z)}{S_{\mathrm{ref}}}\right]\mathrm{dz}$, Z is the depth of 18 kg/m^3 isopycnal, $S(z)$ is salinity as a function of depth, and S_{ref} is a reference salinity taken as 35 pss (Sreelekha et al., 2020). Note that freshwater balance could also be constructed using a CV bounded by a selected isohaline surface (Bryan & Bachman, 2015; Schmitt & Blair, 2015). Net daily freshwater input to BoB within the area enclosed by 18 kg/m^3 isopycnal is given by:

$$\mathrm{FW_{IN}} = \int_A (P + R - E)\,\mathrm{dx}\,\mathrm{dy} \tag{2}$$

where P is precipitation from TRMM, E is evaporation from TropFlux and R is continental discharge from ISBA-CTRIP; for P and E, the integral is over the area A with surface seawater density <18 kg/m^3; the integral of R is evaluated only over that part of the coastline where density of surface seawater <18 kg/m^3 (Figure S1 in Supporting Information S1). The Ganga-Brahmaputra-Meghna (GBM) is the largest of all rivers that discharge

into BoB. Given the significant difference between model GBM river discharge and in situ observations, we choose the grid point at GBM river mouth, and replace the model discharge with in situ GBM discharge data (Papa et al., 2012) to obtain estimates of daily freshwater input for all years. This results in higher June discharge, and peak summer discharge begins to decrease about a week earlier.

Following Wijffels et al. (1992) and Talley (2008), we estimate FWV transport (km^3/day) across the southern boundary of BoB, chosen as 6.5°N from ocean analysis:

$$\mathrm{FW}_T = \int_0^L \int_{-Z(x)}^0 v(x,z)\left[1 - \frac{S(x,z)}{S_{\mathrm{ref}}}\right] \mathrm{dzdx} \tag{3}$$

where L is the width of longitudinal section at 6.5°N, $Z(x)$ is depth of the 18 kg/m^3 isopycnal surface, $v(x, z)$ is meridional velocity at 6.5°N, $S(x, z)$ is salinity at 6.5°N, S_{ref} is 35 pss.

We select 18 kg/m^3 isopycnal surface (which nearly coincides with that of 30 pss isohaline) for constructing freshwater balance for two reasons: First, the area covered by 18 kg/m^3 isopycnal is not significantly affected by spring-time surface warming, unlike the higher values of density. For example, FWV enclosed by the 19 kg/m^3 isopycnal has a distinct secondary peak in April–May. This secondary maximum is mainly due to spring warming of BoB (Sengupta et al., 2002), making the surface water lighter (Figures S2 and S3 in Supporting Information S1). Secondly, the transport of freshwater across the southern boundary within the 18 kg/m^3 CV is zero (Figure S2 in Supporting Information S1)—thus we avoid any errors arising from velocity uncertainties in the ocean analysis data set and need not consider advection across the southern boundary of the bay.

3. Main Results

Sea surface salinity from SMAP and ocean analysis (Figure 1) shows striking seasonality: Surface area covered by the freshest and lightest water in BoB is minimum in April–May and maximum in October–November. Water with salinity <30 pss comes mainly from GBM and Irrawady rivers—it is stirred into the interior by ocean circulation, including mesoscale eddies and wind-driven Ekman flow (Benshila et al., 2014; Sreelekha et al., 2018). Longitude-depth sections show that seawater with potential density <18 kg/m^3 is not transported across the southern boundary of the BoB in any season, in line with climatology (Zweng et al., 2019), multi-year data from surface drifters (Hormann et al., 2019) and glider transects along 8°N east of Sri Lanka (Lee et al., 2016).

Freshwater volume within the 3-dimensional 18 kg/m^3 isopycnal surface (FWV) has similar seasonal dependence to freshwater within the 3-d 30 pss isohaline (Figure 2a). The surface area enclosed by the 18 kg/m^3 and 30 pss isolines are similar, except in winter (Figure 2b). Diminished FWV and area of light water relative to low-salinity water in winter is due to the contribution of temperature to potential density. Mean depth of 18 kg/m^3 and 30 pss isolines are both larger than the mean mixed layer depth (MLD) estimated over the area covered by water lighter than 18 kg/m^3 (Figure 2c). FWV and area within 18 kg/m^3 surface are highly seasonal, with a maximum in October–November, owing to freshwater input to the bay from monsoonal rain and river discharge (Figure 2d) and a minimum in March–May—the ratio of maximum FWV (~2,000 km^3) to minimum FWV (~200 km^3) is nearly 10. In December–February, net surface heat loss from the ocean makes the surface water cooler and denser (Figure 2e)—this is discussed further in Section 3.

The freshwater balance within the 18 kg/m^3 isopycnal surface is given by:

$$\frac{\partial \mathrm{FWV}}{\partial \mathrm{t}} = \mathrm{FW_{IN}} - \mathrm{FW_T} + D \tag{4}$$

where ∂FWV/∂t is the rate of change of freshwater volume, $\mathrm{FW_{IN}}$ is the net input of freshwater, F $\mathrm{W_T}$ is freshwater transport out of the Bay across the southern boundary at 6.5°N and D is a "deficit" term—if continental runoff, surface freshwater flux as well as FWV from ocean analysis were a perfect representation of reality, the deficit term would be entirely due to mixing processes. However, knowledge of each term in the freshwater balance is subject to uncertainty - errors in FWV and net freshwater input are discussed in Section 3.3.

Subseasonal changes in FWC are due to changes in the area enclosed by 18 kg/m^3 isopycnal as the freshwater is advected across the basin by wind-driven flow during active phases of monsoon and mesoscale eddy flow during the break phases of the monsoon (Figure 3a; Sreelekha et al., 2018, 2020). The net input and transport of freshwater within the CV is shown in Figure 3b. The zero transport across the southern boundary of BoB

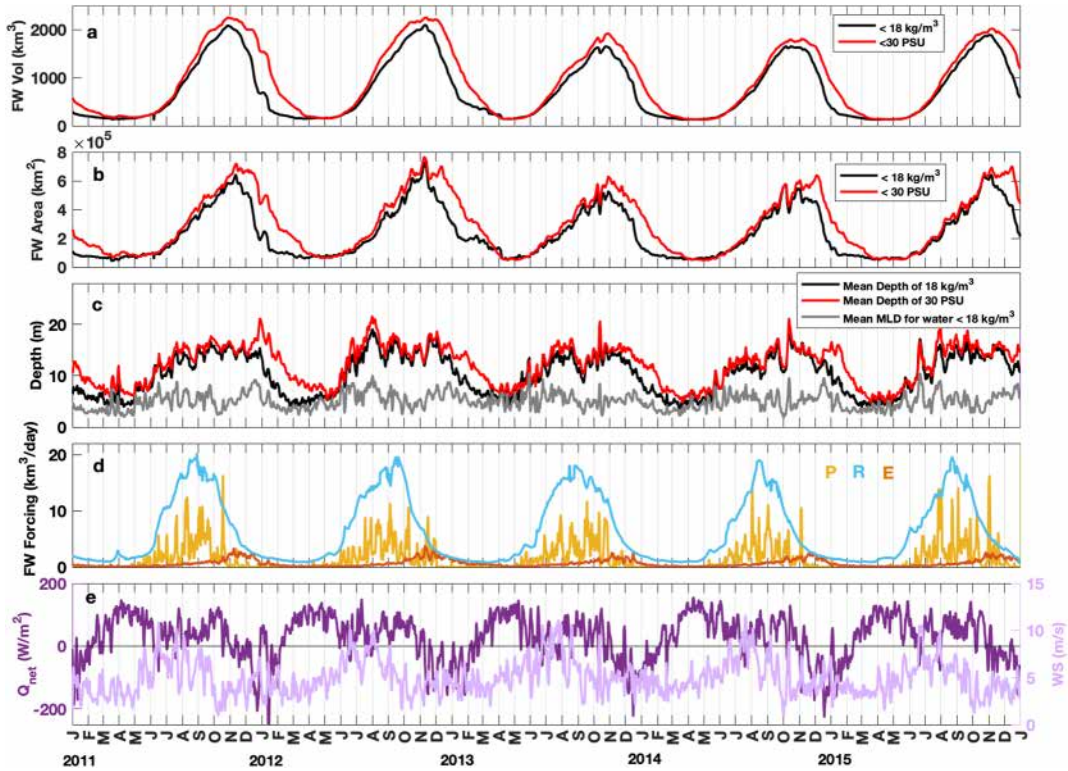

Figure 2. (a) Total freshwater volume (km^3) with salinity <30 pss (black) and potential density <18 kg/m^3 (red). (b) Surface area (km^2) covered by freshwater with salinity <30 pss (black) and density <18 kg/m^3 (red). (c) Mean depth (m) of the 30 pss isohaline surface (black) and the 18 kg/m^3 isopycnal surface (red); mean mixed layer depth (MLD; gray) averaged over all points (x,y) where surface density is less than 18 kg/m^3. (d) TRMM 3B42v7 precipitation (km^3/day; yellow), TropFlux evaporation (km^3/day; orange), ISBA-CTRIP continental river discharge (km^3/day; blue), (e) Tropflux net heat flux (Qnet; W/m^2; purple) and windspeed (m/s; light purple) within the 18 kg/m^3 isopycnal surface.

implies that the freshwater within CV is mixed away entirely within the basin. Figure 3c shows daily FWV and the net accumulation $\int(FW_{IN} - FW_T)\,dt$ within the CV; the time integration during 1 June–31 May each year. In June–July, rise in FWV follows the rise in $\int(FW_{IN} - FW_T)\,dt$ as the net freshwater input to BoB begins to increase. Net freshwater input peaks in August–September, followed by a maximum in FWV about one season later, in October–November. Later, the curve of cumulative freshwater input $\int(FW_{IN} - FW_T)dt$ flattens, indicating that input is relatively small. FWC and FWV decrease rapidly in December–January, reaching a minimum in March–May each year. The deficit or mixing term, obtained by subtracting FWV from cumulative input, is small in June–July and rises gradually in August–October to about 600 km^3 each year, except in 2013 - in that year it reaches nearly 900 km^3, mainly due to widespread enhancement of upper ocean mixing by the intense tropical cyclone Phailin which crossed the northern BoB during 8–12 October (Chaudhuri et al., 2019).

In general, by mid-November and end of January, the deficit term rises steeply by 1,300–2,000 km^3 depending on the year, followed by a modest rise in February–May (Figure 3d). For example, in December 2012, nearly 1,000 km^3 of pure freshwater is lost from the CV in a month. The slope of deficit term is a measure of the rate of mixing of freshwater out of CV. The rate of change of FWC is highest, that is, freshwater loss from the CV is most rapid, in December–January each year. The mean FWC within the CV is generally highest in October to early November, nearly 3.2 m, while the mean rate of freshwater loss in December–January is 0.015 m/day (Figures 3a–3d, Figure S4 in Supporting Information S1).

3.1. Diapycnal Diffusivity in the Bay of Bengal

Following Banyte et al. (2012), the diffusion equation for FWC on isopycnal coordinates is written as:

$$\frac{\partial z}{\partial \rho}\frac{\partial \mathrm{FWC}}{\partial t} = \frac{\partial}{\partial \rho}\left(\kappa \frac{\partial \rho}{\partial z}\frac{\partial \mathrm{FWC}}{\partial \rho}\right) \quad (5)$$

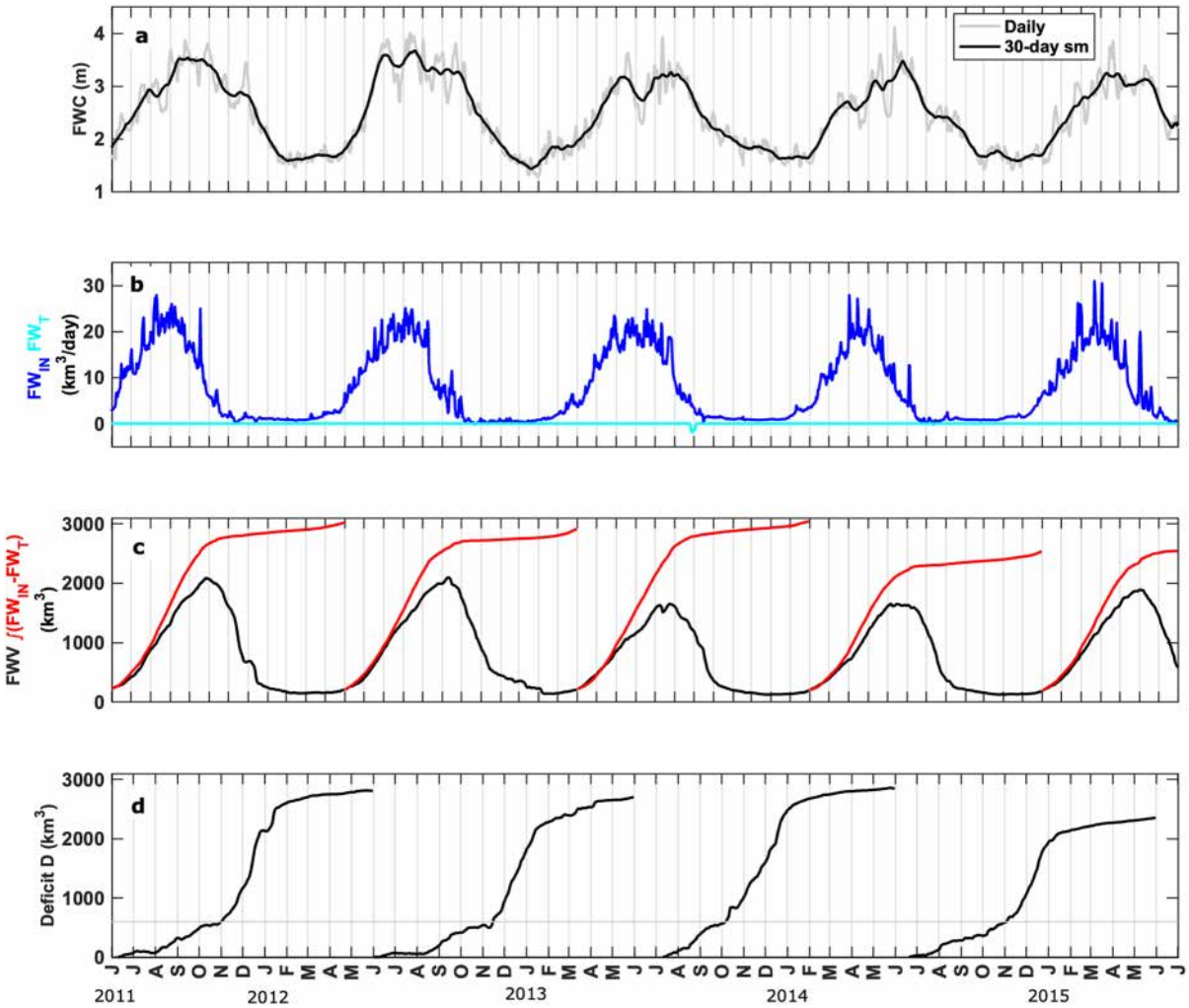

Figure 3. (a) Daily (gray) and 30-day smoothed (black) freshwater content (m), (b) net freshwater input (km^3/day; blue) and net freshwater transport across 6.5°N (km^3/day; cyan) (c) daily freshwater volume (FWV; km^3, black) and net freshwater accumulation ($\int(FW_{IN} - FW_T)\,dt$; km^3, red) estimated from ocean analysis for water with density <18 kg/m^3. (d) Deficit term (km^3) is obtained by subtracting FWV from the net freshwater accumulation shown in (b); estimated error in the deficit term is nearly 25% (thin gray line).

Integrating the above equation from $\rho_{surface}$ to ρ_{18} we get:

$$\frac{\partial \mathrm{FWC}}{\partial t} z_{18} = \kappa \frac{\partial \rho}{\partial z} \frac{\partial \mathrm{FWC}}{\partial \rho} \tag{6}$$

where z_{18} is the depth of 18 kg/m^3 isopycnal, and κ is diapycnal diffusivity across the base of 18 kg/m^3 isopycnal, and $\partial z/\partial \rho$ is spacing between the isopycnals per unit density.

At a given time t, we calculate κ at each grid point (x, y), and then obtain mean diffusivity over the area enclosed by the 18 kg/m^3 isopycnal each day during 2011–2015. As a sensitivity test, we repeated the calculation of the deficit curve and diapycnal diffusivity for water lighter than 18.25 and 18.5 kg/m^3 (Figure 4). In all cases, the highest diffusivities O (10^{-4}) m^2/s are found in winter (December–January), whereas from May to October, the values of κ are of O(10^{-5}) m^2/s. Note that enhanced vertical mixing in the north bay due to the passage of cyclone Phailin, 8–13 October 2013 (Chaudhuri et al., 2019) corresponds to high diffusivities of O(10^{-4}) m^2/s.

3.2. Seasonality in Mixing of Freshwater in the Bay

To examine the seasonality of diffusivity across 18, 18.25, and 18.5 kg/m^3 isopycnals, we calculate probability density function (PDF) of daily estimates of $\log_{10}\kappa$ during summer (June–August), winter (December–January)

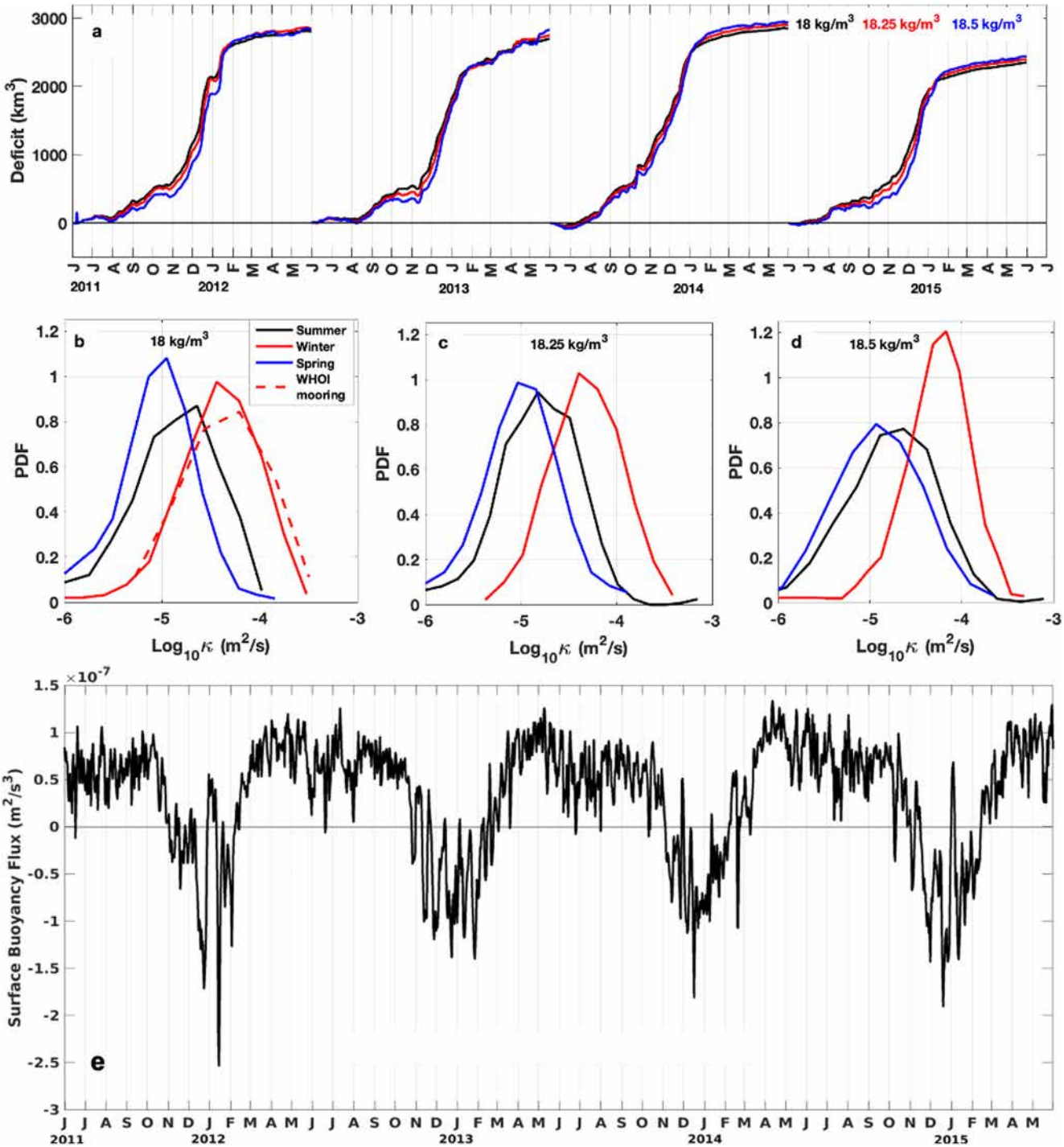

Figure 4. (a) Deficit (km^3) obtained from freshwater balance of water lighter than 18 kg/m^3 (black), 18.25 kg/m^3 (red) and 18.5 kg/m^3 (blue). Probability Density Function (PDF) of derived diffusivity ($\log_{10}\kappa$; m^2/s) within (b) 18 kg/m^3, (c) 18.25 kg/m^3 and (d) 18.5 kg/m^3 isopycnals during summer (June–August; black), winter (December–January; red) and spring (March–May; blue), 2011–2015. PDF of $\log_{10}\kappa$ (m^2/s; red dashed line) in (b) based on χ-pod measurements at 22 m depth at WHOI mooring (18.01°N, 89.45°E), 9 December 2014–31 January 2015. (e) Daily surface buoyancy flux (m^2/s^3) averaged over north of 15°N, June 2011–May 2015.

and spring (March–May) of 2011–2015 (Figures 4b–4d). For 18 kg/m^3 isopycnal, mean diffusivity in summer, winter and spring seasons are 1.4×10^{-5} m^2/s, 5.5×10^{-5} m^2/s, and 1.1×10^{-5} m^2/s respectively; median values are: 0.8×10^{-5} m^2/s, 4.2×10^{-5} m^2/s, and 0.8×10^{-5} m^2/s respectively. In winter, κ exceeds 3×10^{-5} m^2/s about 35% of the time, as compared to 17% and 5% of the time in summer and spring. A distinct shift of winter PDF

toward higher diffusivity values indicates that the highest rates of freshwater mixing occur in December–January, as seen earlier from the rate of change of FWC (Figure 3d). High diapycnal diffusivities in winter are comparable to the diffusivity at 22 m depth at WHOI mooring (18.01°N, 89.45°E) based on χ-pod measurements (Figure 4b; Thakur et al., 2019). In case of 18.25 and 18.5 kg/m^3 isopycnals, the mean diffusivity in each season increases by 10% and 20% respectively as compared to the mean diffusivity across the 18 kg/m^3 isopycnal. As we go to higher density values, we observe significant (60%–80%) increase in the standard deviation of the estimated diffusivity values as compared to 18 kg/m^3 in summer and spring, which is reflected in the broadening of the black and blue PDF curves in Figures 4b–4d. Wintertime PDF becomes more sharply peaked at 18.5 kg/m^3, signifying a smaller spread in diffusivity values (Figure 4d). The reasons require further investigation.

To understand the elevated mixing rates in winter, we examine the role of surface buoyancy flux. Net surface heat flux and latent heat flux from daily TropFlux data set (Praveen Kumar et al., 2012) averaged over BoB north of 15°N show that the ocean loses heat in winter (Figure S5 in Supporting Information S1). In general, mean windspeed over north bay is moderate in spring and winter, and highest during summer monsoon. Latent heat flux, however, is determined by windspeed and humidity gradient q_s–q_a, where q_s is specific humidity at SST and q_a is specific humidity of air near the surface (not shown). Although the humidity gradient and windspeed are comparable in spring and winter (Figure S5 in Supporting Information S1), incident shortwave radiation flux is much higher in spring, giving rise to positive net heat flux (Sengupta et al., 2002).

The net surface buoyancy flux (BF; m^2/s^3) given by:

$$\mathrm{BF} = \frac{g\alpha Q_{\mathrm{net}}}{C_p} - g\beta S(E - P) \tag{7}$$

where g is acceleration due to gravity, α and β are coefficients of thermal expansion and haline contraction, ρ is seawater density, Q_{net} is net surface heat flux, C_p is specific heat of seawater, S is surface salinity, P and E are precipitation and evaporation. BF estimated from ocean analysis, TRMM rainfall and TropFlux surface fluxes shows substantial buoyancy loss from the ocean in November–January every year (Figure 4e). BF estimated from reanalysis and satellite products agrees well with the BF estimated from WHOI mooring measurements during December 2014-December 2015, with a modest bias of -7.2×10^{-9} m^2/s^3 and root-mean-square error (RMSE) of 7.8×10^{-8} m^2/s^3 (Figure S6 in Supporting Information S1). Seasonal reduction in shortwave radiation, and subseasonal episodes of intense cool, dry northeasterly monsoon winds (Figure 2) lead to enhanced surface buoyancy loss in winter (Anitha et al., 2008; Prasad, 1997, 2004).

3.3. Error Analysis

Year-long observations from WHOI mooring at 18oN 89.5°E (Weller et al., 2016) in 2015 are used to validate freshwater content (FWC) estimated from ocean analysis—note that the WHOI mooring observations are not assimilated into ocean analysis. RMSE of FWC at mooring location estimated from ocean analysis is about 0.6 and 0.2 m for 14 and 26 m depth respectively (Figure S7 in Supporting Information S1). In the upper 14 m depth, the error is 10% of the mean FWC estimated from the mooring. Seasonal mean errors are 8.5% in spring, 9.4% in summer and 12.6% in winter. Uncertainties are high during winter as the ocean analysis may not capture the dispersal of low-salinity water coming from the Andaman Sea (Gordon et al., 2017; Sastry et al., 1985). The reliability of ocean analysis subsurface temperature and salinity is likely to be relatively low in the Andaman Sea where Argo float coverage is sparse. Considering an error in the net freshwater input arising from TRMM rainfall, ISBA-CTRIP continental runoff and TropFlux evaporation of 15% (Alkama et al., 2010; Papa et al., 2010; Praveen Kumar et al., 2012; Rahman et al., 2009), the estimated total error in the deficit term (D) is about 25%, that is, only values exceeding 700 km^3 are above the error threshold. The absence of explicit tidal forcing in the ocean model could be a limitation, but tidal effects are present in Argo and sea level data which are assimilated in the analysis.

4. Summary

Very few studies exist of the basin-scale freshwater balance for BoB, which lies in the heart of the south Asian monsoon (Goswami et al., 2016; Sengupta et al., 2006). Using daily three-dimensional ocean analysis, we construct freshwater balance within a control volume bounded by 18 kg/m^3 isopycnal surface for years 2011–2015. We

observe that every year the freshwater with density <18 kg/m^3 is mixed away and converted to higher density class entirely within the bay before it is transported out. The total volume of pure (zero-salinity) freshwater within the CV starts to rise in June, and reaches a maximum in October–November (~2,000 km^3), consistent with accumulation of freshwater during summer monsoon (June–September). Freshwater deficit, defined as the difference between total freshwater volume at any time and cumulative freshwater input, rises most rapidly in December–January each year. Slope of the deficit curve is used to estimate the rate of mixing of freshwater across 18 kg/m^3 surface: We find highest diapycnal diffusivity κ (mean and median values of about 5.5×10^{-5} and 4.2×10^{-5} m^2/s) in December–January. Diapycnal diffusivity in spring and summer seasons are comparable to each other, and nearly four times smaller than in winter. Seasonal reduction of shortwave radiation in winter, and episodes of cool, dry northeast monsoon winds enhance latent heat loss and surface buoyancy loss, making the near-surface layer unstable (Prasad, 2004). We propose that winter-time convective mixing driven by surface buoyancy loss reduces freshwater content at a mean rate of 0.015 m/day. The basin-scale wintertime diapycnal diffusivity estimated from freshwater balance is consistent with direct χ-pod measurements at WHOI mooring (18 N, 89.5 E) in BoB. This study has implications for improvement of ocean and climate models, which generally have too-high mixing rates and poor representation of the salinity-stratified near-surface layer in BoB. More detailed knowledge of mixing is important for climate and ocean biogeochemistry, but our understanding of the mechanisms of turbulent mixing remains a challenge due to limited availability of long-term, high-resolution observations in the near-surface BoB.

Data Availability Statement

The data sets used in this study are publicly available: GLOBAL_MULTIYEAR_PHY_001_030 EU (2023); TropFlux data available at Praveen Kumar et al. (2012); TRMM 3B42v7 precipitation at Huffman et al. (2016); ISBA-CTRIP continental runoff data is available at Jarugula and Decharme (2023).

Acknowledgments
This research was conducted while SJ was at IISc, Bangalore. We acknowledge Ministry of Earth Sciences (MoES), National Monsoon Mission, Indian Institute of Tropical Meteorology for support through Ocean Mixing and Monsoon (OMM) and the Office of Naval Research through grant N00014-17-1-2472 and Research Opportunities for Program Officers program. We are grateful to Prof. Amit Tandon for many discussions and valuable insight. We thank Dr. Fabien Durand for several useful suggestions, and Dr. Bertrand Decharme for guidance on continental runoff data. Views presented herein are those of E. Shroyer and do not necessarily represent the views of US DoD or its components.

References

Adams, K., MacKinnon, J., Lucas, A. J., Nash, J., Shroyer, E., & Farrar, J. T. (2019). Multi-platform observations of small-scale lateral mixed layer variability in the northern Bay of Bengal. *Deep Sea Research Part II: Topical Studies in Oceanography*, *168*, 104629. https://doi.org/10.1016/j.dsr2.2019.07.017

Akhil, V. P., Durand, F., Lengaigne, M., Vialard, J., Keerthi, M. G., Gopalakrishna, V. V., et al. (2014). A modeling study of the processes of surface salinity seasonal cycle in the Bay of Bengal. *Journal of Geophysical Research: Oceans*, *119*(6), 3926–3947. https://doi.org/10.1002/2013jc009632

Alkama, R., Decharme, B., Douville, H., Becker, M., Cazenave, A., Sheffield, J., et al. (2010). Global evaluation of the ISBA-TRIP continental hydrological system. Part I: Comparison to GRACE terrestrial water storage estimates and in situ river discharges. *Journal of Hydrometeorology*, *11*(3), 583–600. https://doi.org/10.1175/2010jhm1211.1

Anitha, G., Ravichandran, M., & Sayanna, R. (2008). Surface buoyancy flux in Bay of Bengal and Arabian Sea. *Annales Geophysicae*, *26*(3), 395–400. https://doi.org/10.5194/angeo-26-395-2008

Balaguru, K., Chang, P., Saravanan, R., Leung, L. R., Xu, Z., Li, M., & Hsieh, J. S. (2012). Ocean barrier layers' effect on tropical cyclone intensification. *Proceedings of the National Academy of Sciences of the United States of America*, *109*(36), 14343–14347. https://doi.org/10.1073/pnas.1201364109

Banyte, D., Tanhua, T., Visbeck, M., Wallace, D. W., Karstensen, J., Krahmann, G., et al. (2012). Diapycnal diffusivity at the upper boundary of the tropical North Atlantic oxygen minimum zone. *Journal of Geophysical Research*, *117*(C9), C09016. https://doi.org/10.1029/2011jc007762

Benshila, R., Durand, F., Masson, S., Bourdallé-Badie, R., de Boyer Montégut, C., Papa, F., & Madec, G. (2014). The upper Bay of Bengal salinity structure in a high-resolution model. *Ocean Modelling*, *74*, 36–52. https://doi.org/10.1016/j.ocemod.2013.12.001

Bhat, G. S., Gadgil, S., Kumar, P. H., Kalsi, S. R., Madhusoodanan, P., Murty, V. S. N., et al. (2001). BAY OF BENGAL MEX: The Bay of Bengal monsoon experiment. *Bulletin of the American Meteorological Society*, *82*(10), 2217–2244.

Blanke, B., & Delecluse, P. (1993). Variability of the tropical Atlantic Ocean simulated by a general circulation model with two different mixed-layer physics. *Journal of Physical Oceanography*, *23*(7), 1363–1388. https://doi.org/10.1175/1520-0485(1993)023<1363:vottao>2.0.co;2

Bryan, F., & Bachman, S. (2015). Isohaline salinity budget of the North Atlantic salinity maximum. *Journal of Physical Oceanography*, *45*(3), 724–736. https://doi.org/10.1175/jpo-d-14-0172.1

Chassignet, E., Pascual, A., Tintore, J., & Verron, J. (2018). *New frontiers in operational oceanography*. GODAE Oceanview.

Chaudhuri, D., Sengupta, D., D'Asaro, E., & Shivaprasad, S. (2021). Trapping of wind momentum in a salinity-stratified ocean. *Journal of Geophysical Research: Oceans*, *126*(12), e2021JC017770. https://doi.org/10.1029/2021jc017770

Chaudhuri, D., Sengupta, D., D'Asaro, E., Venkatesan, R., & Ravichandran, M. (2019). Response of the salinity-stratified Bay of Bengal to cyclone Phailin. *Journal of Physical Oceanography*, *49*(5), 1121–1140. https://doi.org/10.1175/jpo-d-18-0051.1

Cherian, D. A., Shroyer, E. L., Wijesekera, H. W., & Moum, J. N. (2020). The seasonal cycle of upper ocean mixing at 8°N in the Bay of Bengal. *Journal of Physical Oceanography*, *50*(2), 323–342. https://doi.org/10.1175/jpo-d-19-0114.1

Decharme, B., Alkama, R., Papa, F., Faroux, S., Douville, H., & Prigent, C. (2012). Global off-line evaluation of the ISBA-TRIP flood model. *Climate Dynamics*, *38*(7–8), 1389–1412. https://doi.org/10.1007/s00382-011-1054-9

Decharme, B., Delire, C., Minvielle, M., Colin, J., Vergnes, J. P., Alias, A., et al. (2019). Recent changes in the ISBA-CTRIP land surface system for use in the CNRM-CM6 climate model and in global off-line hydrological applications. *Journal of Advances in Modeling Earth Systems*, *11*(5), 1207–1252. https://doi.org/10.1029/2018ms001545

E.U. (2023). Copernicus marine service information (CMEMS) [Dataset]. Marine Data Store (MDS) GLOBAL_MULTIYEAR_PHY_001_030. https://doi.org/10.48670/moi-00021

Fu, X., Wang, B., Waliser, D. E., & Tao, L. (2007). Impact of atmosphere–ocean coupling on the predictability of monsoon intraseasonal oscillations. *Journal of the Atmospheric Sciences*, *64*(1), 57–174. https://doi.org/10.1175/jas3830.1

Gadgil, S. (2003). The Indian monsoon and its variability. *Annual Review of Earth and Planetary Sciences*, *31*(1), 429–467. https://doi.org/10.1146/annurev.earth.31.100901.141251

George, J. V., Vinayachandran, P. N., Vijith, V., Thushara, V., Nayak, A. A., Pargaonkar, S. M., et al. (2019). Mechanisms of barrier layer formation and erosion from in situ observations in the Bay of Bengal. *Journal of Physical Oceanography*, *49*(5), 1183–1200. https://doi.org/10.1175/jpo-d-18-0204.1

Girishkumar, M. S., Ashin, K., McPhaden, M. J., Balaji, B., & Praveenkumar, B. (2020). Estimation of vertical heat diffusivity at the base of the mixed layer in the Bay of Bengal. *Journal of Geophysical Research: Oceans*, *125*(5), e2019JC015402. https://doi.org/10.1029/2019jc015402

Gordon, A. L., Shroyer, E., & Murty, V. S. N. (2017). An intrathermocline eddy and a tropical cyclone in the Bay of Bengal. *Scientific Reports*, *7*(1), 46218. https://doi.org/10.1038/srep46218

Goswami, B. N., Rao, S. A., Sengupta, D., & Chakravorty, S. (2016). Monsoons to mixing in the Bay of Bengal: Multiscale air-sea interactions and monsoon predictability. *Oceanography*, *29*(2), 18–27. https://doi.org/10.5670/oceanog.2016.35

Gregg, M. C., D'Asaro, E. A., Riley, J. J., & Kunze, E. (2018). Mixing efficiency in the ocean. *Annual Review of Marine Science*, *10*(1), 443–473. https://doi.org/10.1146/annurev-marine-121916-063643

Hormann, V., Centurioni, L. R., & Gordon, A. L. (2019). Freshwater export pathways from the Bay of Bengal. *Deep Sea Research Part II: Topical Studies in Oceanography*, *168*, 104645. https://doi.org/10.1016/j.dsr2.2019.104645

Huffman, G. J., Bolvin, D. T., Nelkin, E. J., & Adler, R. F. (2016). TRMM (TMPA) Precipitation L3 1 day 0.25 degree x 0.25 degree V7 [Dataset]. In A. Savtchenko (Eds.), *Goddard Earth sciences data and information services center (GES DISC)*. https://doi.org/10.5067/TRMM/TMPA/DAY/7

Jampana, V., Ravichandran, M., Sengupta, D., D'Asaro, E. A., Rahaman, H., Joseph, S., et al. (2018). Shear flow instabilities and unstable events over the North Bay of Bengal. *Journal of Geophysical Research: Oceans*, *123*(12), 8958–8969. https://doi.org/10.1029/2017jc013272

Jarugula, S., & Decharme, B. (2023). Daily continental discharge data for Bay of Bengal [Dataset]. Zenodo. https://doi.org/10.5281/zenodo.10369268

Lau, W. K. M., Waliser, D. E., & Goswami, B. N. (2012). South Asian monsoon. In *Intraseasonal variability in the atmosphere-ocean climate system* (pp. 21–72). Springer.

Lee, C. M., Jinadasa, S. U. P., Anutaliya, A., Centurioni, L. R., Fernando, H. J., Hormann, V., et al. (2016). Collaborative observations of boundary currents, water mass variability, and monsoon response in the southern Bay of Bengal. *Oceanography*, *29*(2), 102–111. https://doi.org/10.5670/oceanog.2016.43

Lucas, A. J., Nash, J. D., Pinkel, R., MacKinnon, J. A., Tandon, A., Mahadevan, A., et al. (2016). Adrift upon a salinity-stratified sea: A view of upper-ocean processes in the Bay of Bengal during the southwest monsoon. *Oceanography*, *29*(2), 134–145. https://doi.org/10.5670/oceanog.2016.46

Mahadevan, A., Paluszkiewicz, T., Ravichandran, M., Sengupta, D., & Tandon, A. (2016). Introduction to the special issue on the Bay of Bengal: From monsoons to mixing. *Oceanography*, *29*(2), 14–17. https://doi.org/10.5670/oceanog.2016.34

Moum, J. N. (2021). Variations in ocean mixing from seconds to years. *Annual Review of Marine Science*, *13*(1), 201–226. https://doi.org/10.1146/annurev-marine-031920-122846

Moum, J. N., & Smyth, W. D. (2001). Upper ocean mixing. *Encyclopedia of Ocean Sciences*, *6*, 3093–3100.

Munk, W., & Wunsch, C. (1998). Abyssal recipes II: Energetics of tidal and wind mixing. *Deep Sea Research Part I: Oceanographic Research Papers*, *45*(12), 1977–2010. https://doi.org/10.1016/s0967-0637(98)00070-3

Neetu, S., Lengaigne, M., Vincent, E. M., Vialard, J., Madec, G., Samson, G., et al. (2012). Influence of upper-ocean stratification on tropical cyclone-induced surface cooling in the Bay of Bengal. *Journal of Geophysical Research*, *117*(C12), C12020. https://doi.org/10.1029/2012jc008433

Papa, F., Bala, S. K., Pandey, R. K., Durand, F., Gopalakrishna, V. V., Rahman, A., & Rossow, W. B. (2012). Ganga-Brahmaputra River discharge from Jason-2 radar altimetry: An update to the long-term satellite-derived estimates of continental freshwater forcing flux into the Bay of Bengal. *Journal of Geophysical Research*, *117*(C11), C11021. https://doi.org/10.1029/2012jc008158

Papa, F., Durand, F., Rossow, W. B., Rahman, A., & Bala, S. K. (2010). Satellite altimeter-derived monthly discharge of the Ganga-Brahmaputra River and its seasonal to interannual variations from 1993 to 2008. *Journal of Geophysical Research*, *115*(C12), C12013. https://doi.org/10.1029/2009jc006075

Prasad, T. G. (1997). *Annual and seasonal mean buoyancy fluxes for the tropical Indian Ocean* (pp. 667–674). Current Science.

Prasad, T. G. (2004). A comparison of mixed-layer dynamics between the Arabian Sea and Bay of Bengal: One-dimensional model results. *Journal of Geophysical Research*, *109*(C3), C03035. https://doi.org/10.1029/2003jc002000

Praveen Kumar, B., Vialard, J., Lengaigne, M., Murty, V. S. N., & Mcphaden, M. J. (2012). TropFlux: Air-sea fluxes for the global tropical oceans—Description and evaluation [Dataset]. Climate Dynamics, *38*(7–8), 1521–1543. https://doi.org/10.1007/s00382-011-1115-0

Rahman, S. H., Sengupta, D., & Ravichandran, M. (2009). Variability of Indian summer monsoon rainfall in daily data from gauge and satellite. *Journal of Geophysical Research*, *114*(D17), D17113. https://doi.org/10.1029/2008jd011694

Samanta, D., Hameed, S. N., Jin, D., Thilakan, V., Ganai, M., Rao, S. A., & Deshpande, M. (2018). Impact of a narrow coastal Bay of Bengal sea surface temperature front on an Indian summer monsoon simulation. *Scientific Reports*, *8*(1), 1–12. https://doi.org/10.1038/s41598-018-35735-3

Sastry, J. S., Rao, D. P., Murty, V. S. N., Sarma, Y. V. B., Suryanarayana, A., & Babu, M. T. (1985). Watermass structure in the bay of Bengal. Mahasagar. *Bulletin of the National Institute of Oceanography*, *18*, 153–162.

Schmitt, R., & Blair, A. (2015). A river of salt. *Oceanography*, *28*(1), 40–45. https://doi.org/10.5670/oceanog.2015.04

Sengupta, D., Bharath Raj, G. N., & Shenoi, S. S. C. (2006). Surface freshwater from Bay of Bengal runoff and Indonesian throughflow in the tropical Indian Ocean. *Geophysical Research Letters*, *33*(22), L22609. https://doi.org/10.1029/2006gl027573

Sengupta, D., Ray, P. K., & Bhat, G. S. (2002). Spring warming of the eastern Arabian Sea and Bay of Bengal from buoy data. *Geophysical Research Letters*, *29*(15), 24–1. https://doi.org/10.1029/2002gl015340

Shroyer, E., Tandon, A., Sengupta, D., Fernando, H. J., Lucas, A. J., Farrar, J. T., et al. (2021). Bay of Bengal intraseasonal oscillations and the 2018 monsoon onset. *Bulletin of the American Meteorological Society*, *102*(10), E1936–E1951. https://doi.org/10.1175/bams-d-20-0113.1

Shroyer, E. L., Rudnick, D. L., Farrar, J. T., Lim, B., Venayagamoorthy, S. K., St. Laurent, L. C., et al. (2016). Modification of upper-ocean temperature structure by subsurface mixing in the presence of strong salinity stratification. *Oceanography*, *29*(2), 62–71. https://doi.org/10.5670/oceanog.2016.39

Sreelekha, J., Buckley, J. M., Tandon, A., & Sengupta, D. (2018). Subseasonal dispersal of freshwater in the northern Bay of Bengal in the 2013 summer monsoon season. *Journal of Geophysical Research: Oceans*, *123*(9), 6330–6348. https://doi.org/10.1029/2018jc014181

Sreelekha, J., Lucas, A. J., Sukhatme, J., Joseph, J. K., Ravichandran, M., Suresh Kumar, N., et al. (2020). Quasi-biweekly mode of the Asian summer monsoon revealed in Bay of Bengal surface observations. *Journal of Geophysical Research: Oceans*, *125*(12), e2020JC016271. https://doi.org/10.1029/2020jc016271

Talley, L. D. (2008). Freshwater transport estimates and the global overturning circulation: Shallow, deep and throughflow components. *Progress in Oceanography*, *78*(4), 257–303. https://doi.org/10.1016/j.pocean.2008.05.001

Thadathil, P., Suresh, I., Gautham, S., Prasanna Kumar, S., Lengaigne, M., Rao, R. R., et al. (2016). Surface layer temperature inversion in the Bay of Bengal: Main characteristics and related mechanisms. *Journal of Geophysical Research: Oceans*, *121*(8), 5682–5696. https://doi.org/10.1002/2016jc011674

Thakur, R., Shroyer, E. L., Govindarajan, R., Farrar, J. T., Weller, R. A., & Moum, J. N. (2019). Seasonality and buoyancy suppression of turbulence in the Bay of Bengal. *Geophysical Research Letters*, *46*(8), 4346–4355. https://doi.org/10.1029/2018gl081577

Vecchi, G. A., & Harrison, D. E. (2002). Monsoon breaks and subseasonal sea surface temperature variability in the Bay of Bengal. *Journal of Climate*, *15*(12), 1485–1493. https://doi.org/10.1175/1520-0442(2002)015<1485:mbasss>2.0.co;2

Vinayachandran, P. N., Murty, V. S. N., & Ramesh Babu, V. (2002). Observations of barrier layer formation in the Bay of Bengal during summer monsoon. *Journal of Geophysical Research*, *107*(C12), SRF19-1–SRF19-9. https://doi.org/10.1029/2001jc000831

Vinayachandran, P. N., Shankar, D., Vernekar, S., Sandeep, K. K., Amol, P., Neema, C. P., & Chatterjee, A. (2013). A summer monsoon pump to keep the Bay of Bengal salty. *Geophysical Research Letters*, *40*(9), 1777–1782. https://doi.org/10.1002/grl.50274

Warner, S. J., Becherer, J., Pujiana, K., Shroyer, E. L., Ravichandran, M., Thangaprakash, V. P., & Moum, J. N. (2016). Monsoon mixing cycles in the Bay of Bengal: A year-long subsurface mixing record. *Oceanography*, *29*(2), 158–169. https://doi.org/10.5670/oceanog.2016.48

Webster, P. J. (2006). The coupled monsoon system. In *The Asian monsoon* (pp. 3–66). Springer.

Weller, R. A., Farrar, J. T., Buckley, J., Mathew, S., Venkatesan, R., Lekha, J. S., et al. (2016). Air-sea interaction in the Bay of Bengal. *Oceanography*, *29*(2), 28–37. https://doi.org/10.5670/oceanog.2016.36

Wijesekera, H. W., Shroyer, E., Tandon, A., Ravichandran, M., Sengupta, D., Jinadasa, S., et al. (2016). ASIRI: An ocean–atmosphere initiative for Bay of Bengal. *Bulletin of the American Meteorological Society*, *97*(10), 1859–1884. https://doi.org/10.1175/bams-d-14-00197.1

Wijffels, S. E., Schmitt, R. W., Bryden, H. L., & Stigebrandt, A. (1992). Transport of freshwater by the oceans. *Journal of Physical Oceanography*, *22*(2), 155–162. https://doi.org/10.1175/1520-0485(1992)022<0155:tofbto>2.0.co;2

Wilson, E. A., & Riser, S. C. (2016). An assessment of the seasonal salinity budget for the upper Bay of Bengal. *Journal of Physical Oceanography*, *46*(5), 1361–1376. https://doi.org/10.1175/jpo-d-15-0147.1

Zweng, M. M., Seidov, D., Boyer, T. P., Locarnini, M., Garcia, H. E., Mishonov, A. V., et al. (2019). In *World ocean atlas 2018* (Vol. 2). Salinity.